

Optogenetic manipulation of medullary neurons in the locust optic lobe

Hongxia Wang,¹  Richard B. Dewell,¹ Markus U. Ehrenguber,² Eran Segev,³ Jacob Reimer,¹ Michael L. Roukes,³ and  Fabrizio Gabbiani^{1,4}

¹Department of Neuroscience, Baylor College of Medicine, Houston, Texas; ²Department of Biology, Kantonsschule Hohe Promenade, Zurich, Switzerland; ³Department of Applied Physics and Material Science, California Institute of Technology, Pasadena, California; and ⁴Electrical and Computer Engineering Department, Rice University, Houston, Texas

Submitted 31 May 2018; accepted in final form 9 August 2018

Wang H, Dewell RB, Ehrenguber MU, Segev E, Reimer J, Roukes ML, Gabbiani F. Optogenetic manipulation of medullary neurons in the locust optic lobe. *J Neurophysiol* 120: 2049–2058, 2018. First published August 15, 2018; doi:10.1152/jn.00356.2018.—The locust is a widely used animal model for studying sensory processing and its relation to behavior. Due to the lack of genomic information, genetic tools to manipulate neural circuits in locusts are not yet available. We examined whether Semliki Forest virus is suitable to mediate exogenous gene expression in neurons of the locust optic lobe. We subcloned a channelrhodopsin variant and the yellow fluorescent protein Venus into a Semliki Forest virus vector and injected the virus into the optic lobe of locusts (*Schistocerca americana*). Fluorescence was observed in all injected optic lobes. Most neurons that expressed the recombinant proteins were located in the first two neuropils of the optic lobe, the lamina and medulla. Extracellular recordings demonstrated that laser illumination increased the firing rate of medullary neurons expressing channelrhodopsin. The optogenetic activation of the medullary neurons also triggered excitatory postsynaptic potentials and firing of a postsynaptic, looming-sensitive neuron, the lobula giant movement detector. These results indicate that Semliki Forest virus is efficient at mediating transient exogenous gene expression and provides a tool to manipulate neural circuits in the locust nervous system and likely other insects.

NEW & NOTEWORTHY Using Semliki Forest virus, we efficiently delivered channelrhodopsin into neurons of the locust optic lobe. We demonstrate that laser illumination increases the firing of the medullary neurons expressing channelrhodopsin and elicits excitatory postsynaptic potentials and spiking in an identified postsynaptic target neuron, the lobula giant movement detector neuron. This technique allows the manipulation of neuronal activity in locust neural circuits using optogenetics.

LGMD; locust; medulla; optogenetics; Semliki Forest virus

INTRODUCTION

Insects are widely used to address fundamental questions about brain mechanisms. Research on insects has broadened our knowledge and helped us understand the neural bases of complex behavior, e.g., communication and navigation in bees and ants (Evangalista et al. 2014; Srinivasan 2010; Wehner 2003), vision and motion detection in flies (Egelhaaf 2008),

olfactory learning and odor discrimination in sphinx moths, locusts, and flies (Gupta and Stopfer 2011), auditory processing in crickets (Göpfert and Hennig 2016), as well as the mechanisms of neural development and genetics, most recently mainly in *Drosophila* (Hales et al. 2015; Spindler and Hartenstein 2010). In these endeavors, genetic tools are helpful for dissecting neural circuits and deciphering the neural mechanisms underlying different behaviors. Since most neurons in *Drosophila* are small, they are unsuitable for intracellular dendritic recordings, making this genetic model system of limited use for investigations of dendritic computations in single cells. On the other hand, insects with larger neurons, such as locusts, crickets, and moths, have proved optimal for intracellular electrophysiological recordings. In most of these insects, however, it is not easy to manipulate gene expression and carry out genome editing due to lack of genome sequencing information and long generation times. Nevertheless, researchers have developed a variety of genetic tools for several such species. For example, *piggyBac*-derived cassettes have been integrated in the honeybee (*Apis mellifera*) expressing the fluorescent markers Rubia and enhanced green fluorescent protein (eGFP) under either an artificial or an endogenous promoter (Schulte et al. 2014). In two other cases, odorant receptor coreceptor (orco) mutated ant and locust germ lines have been generated in *Ooceraea biroi* and *Locusta migratoria* by using CRISPR/Cas9 gene editing technology (Li et al. 2016; Tribble et al. 2017).

The locust is a popular model for studying behavior relying on visual motion, especially visually evoked escape and collision avoidance behavior (Fotowat and Gabbiani 2011). Creating transgenic locust germ lines or developing an efficient transfection method in locusts to deliver neuronal activity indicators or modulators would be desirable to increase the power of this model system. However, up to now, there are no known reports on such foreign transformations in the nervous system of locusts. Optogenetics is an efficient stimulation method to control neuronal activity using light-gated ion channels such as channelrhodopsin, halorhodopsin, and their variants (Arrenberg et al. 2009; Boyden et al. 2005; Ishizuka et al. 2006). It has been broadly used to map neural circuitry, study neuronal activity, control cardiac function, and treat photoreceptor degeneration and Parkinson's disease (Adamantidis et al. 2007; Arenkiel et al. 2007; Bi et al. 2006; Gradinaru et al. 2009).

Address for reprint requests and other correspondence: F. Gabbiani, Dept. of Neuroscience, Baylor College of Medicine, One Baylor Plaza, Houston, TX 77030 (e-mail: gabbiani@bcm.edu).

Semliki Forest virus (SFV) is an enveloped single-stranded, positive RNA virus, one of the members in the alphavirus family (Strauss and Strauss 1994). In earlier work, wild-type SFV and mutant SFV A7(74) were used to drive LacZ and GFP expressions in pyramidal neurons of cultured hippocampal slices (Ehrengruber et al. 1999 2003). Similarly, the less cytopathic mutant SFV(PD) (Lundstrom et al. 2003) drove protein expression in the rat calyx of Held in vivo (Wimmer et al. 2004). Since SFV is a mosquito-borne pathogen, it could possibly infect other nonhost insect cells (Lwande et al. 2013), as has been shown for the Sindbis virus (Lewis et al. 1999). To test the possibility that SFV could drive foreign gene expression in locust neurons, we inserted into a SFV A7(74)-based vector (Ehrengruber et al. 2003) the channelrhodopsin variant Chop-Wide Receiver (ChopWR), tagged with a fluorescent marker Venus (Wang et al. 2009) downstream of a strong ubiquitous promoter. ChopWR is a chimeric protein of Chop1 and Chop2 (Nagel et al. 2003), consisting of the first to fifth transmembrane domains from Chop1 and the sixth to seventh transmembrane domains from Chop2. ChopWR was extensively characterized by Wang et al. (2009) and has several advantages over Chop2. For example, ChopWR has improved membrane expression, mediating a larger photocurrent with decreased desensitization and a wider absorption spectrum (Wang et al. 2009). ChopWR has been used, e.g., to study courtship behavior in *Drosophila* and escape behavior in zebrafish (Kohatsu and Yamamoto 2015; Umeda et al. 2013). The plasmid containing the ChopWR-Venus gene was electroporated into baby hamster kidney 21 (BHK-21) cells for generating the virus, which was injected through the eye into the optic lobe of locusts.

In this paper, we show that viral replicons based on the SFV A7(74) strain successfully express ChopWR-Venus in medullary neurons of the locust optic lobe, enabling us to manipulate optogenetically their activity and that of the lobula giant movement detector (LGMD), a downstream neuron that plays a vital role in collision avoidance behavior (Fotowat and Gabbiani 2011).

MATERIALS AND METHODS

Generation of SFV vectors encoding ChopWR-Venus. The practical steps for the generation of SFV vectors were described in previous papers (e.g., Ehrengruber et al. 2011). The fabrication method follows that developed by Liljeström and Garoff (1991). It relies on an expression plasmid (i.e., “vector” plasmid) encoding the SFV nonstructural proteins and the foreign gene of interest (transgene), while a second plasmid (i.e., “helper” plasmid) is used to synthesize the viral structural proteins required for the packaging of the SFV particles. Upon in vitro transcription of vector and helper RNA, both RNAs are electroporated into secondary tissue cultures, e.g., BHK-21 cells, for SFV protein synthesis and virus assembly. Because the viral packaging signal is present in the vector rather than in the helper RNA, only vector RNA is packaged into recombinant viral particles, termed “replicons”. Upon subsequent infection of a target cell, replicons will replicate their viral RNA genome without generating new infectious particles (due to the lack of the necessary SFV capsid and spike proteins). This approach provides the biosafety properties that are typical of the expression systems based on SFV and other alphaviruses, such as the Sindbis virus, and the resulting viral replicons have therefore been termed “suicide vectors” (Schlesinger 1993). As an additional safety feature for SFV vectors, the viral particles were designed to be conditionally infectious due to the requirement of unphysiologically high chymotrypsin concentrations for their activa-

tion, i.e., cleavage of the spike precursor protein, as described by Berglund et al. (1993).

For the present study, the ChopWR-Venus gene was first subcloned into the pENTR2B entry vector and then transferred to the pScaA7-RFA destination vector by using the attB1 and attB2 attachment sites through Gateway Technology (Thermo Fisher Scientific, Waltham, MA). The destination vector pScaA7-RFA was obtained from a modified SFV A7(74) vector plasmid, pSFV(A774nsP) (Ehrengruber et al. 2003), by moving A7(74)nsP1–4 into the pSCA plasmid (DiCiommo and Bremner 1998). This plasmid uses the cytomegalovirus (CMV)/T7 promoters instead of the SP6 promoter and is compatible with Gateway Technology. The plasmid map of the pScaA7-RFA vector containing ChopWR-Venus is illustrated in Fig. 1A. The ChopWR-Venus gene was inserted downstream of the endogenous SFV subgenomic promoter that follows the sequence of the SFV nonstructural proteins 1–4 (nsP1–4). Unique restriction sites are indicated in Fig. 1A, as is the simian virus 40 polyadenylation (SV40 polyA) terminator sequence, the Ampicillin resistance gene, and the pBR322 origin of replication. The resulting plasmid and the auxiliary plasmid pSFV-helper2 were purified and linearized with the restriction enzyme *SpeI* (New England Biolabs, Ipswich, MA; NEB). The pENTR2B and pScaA7 plasmids were a gift from Dr. Keith Murai (McGill University, Montreal, Canada) and the pSFV-helper2 plasmid was a gift of Dr. Alan L. Goldin (University of California, Irvine, CA).

Next, T7 and Sp6 RNA polymerase (Thermo Fisher Scientific) were used to catalyze the formation of RNAs from linearized pScaA7-ChopWR-Venus and pSFV-helper2 DNAs, respectively. To produce viruses, in vitro-transcribed RNA from pScaA7-ChopWR-Venus and pSFV-helper2 were coelectroporated into BHK-21 cells. After that, BHK-21 cells were incubated for 24–48 h in minimum essential (α -MEM) medium containing 5% fetal bovine serum (FBS) at 31°C with 5% CO₂ (Thermo Fisher Scientific). After 48 h, the virus containing supernatant was filtered with a Nalgene filter unit (0.2 μ m, with PES membrane) and concentrated in a Spin-X UF concentrator (Corning, Corning, NY) by centrifugation for 30 min at room temperature (3,000 rpm). For viral stock production, the harvested SFV replicons were activated by 500 μ g/ml α -chymotrypsin for 30 min at room temperature, and the reaction was stopped by 250 μ g/ml aprotinin (Sigma-Aldrich, St. Louis, MO).

Virus titer determination. The harvested SFV stocks were gradually diluted 10, 100, 1,000, 1×10^4 , 1×10^5 , or 1×10^6 times with α -MEM containing 5% FBS. One milliliter of virus solution from each dilution was added to cultured BHK-21 cells. The BHK-21 cells were incubated with the virus for 1 h at 37°C. To ensure that the virus solution entered into contact with the cells, the culture plate was gently rocked every 15 min. Thereafter, the BHK-21 cells were incubated for another 24 h at 37°C upon adding α -MEM (containing 1% FBS). After 24 h, viral transduction was checked visually (based on Venus fluorescence) in all cultures, and the viral titer was calculated by counting the number of fluorescent cells present at the highest dilution multiplied by the dilution factor. The SFV virus titers used in subsequent experiments were $\sim 1 \times 10^5$ infectious particles per milliliter. All protocols were approved by the Bio-Environmental Safety Committee of Baylor College of Medicine.

Injection of the viral solution into locusts. Experiments were done using both male and female locusts, *Schistocerca americana*, 8–10 wk old. Before virus injection, the locusts were fed for 2 days in the dark with grass sprayed using an aqueous solution containing *all-trans*-retinal initially dissolved in 1 ml of ethanol (final concentration: 1 mM; Toronto Research Chemicals, North York, ON, Canada). Locusts were immobilized by wrapping them in tissue paper and taping them into a custom-made rectangular plastic holder. The holder was placed under a stereomicroscope (Leica MZ7.5), and the eye was visualized at a total magnification of about $\times 50$. A sharp probe was used to make a hole in the middle of the right eye between the third and fifth dark stripes. A volume of 1–2 μ l of viral solution was

injected through this hole using a glass pipette mounted on a micro-manipulator with positive pressure generated using a 1-ml syringe. The glass pipette was prepared on a Sutter P87 puller, using a thin glass capillary (TW120F-4; WPI, Sarasota, FL) and had a final tip diameter of 2–5 μm . The depth of injection was ~ 450 – 700 μm . For further details on drug injections through the eye, see Dewell and Gabbiani (2018). Although we did not quantify this systematically, we observed that the level of expression depended on the depth and location of injection as well as on the titer of the virus. All protocols

were approved by the Bio-Environmental Safety Committee of Baylor College of Medicine.

Pilot experiments with other virus expression systems. In preliminary experiments, we tested several additional viral delivery vectors. Sindbis virus with the SP6 promoter was prepared similarly as described above. The titer for Sindbis virus was 5×10^6 infectious particles per milliliter. Recombinant, GFP-tagged baculovirus with the polyhedrin promoter was purchased from a commercial supplier (no. C14, AB Vector; titer: 10^8 pfu/ml). Recombinant adeno-associated virus (AAV)-eGFP with the CMV promoter was a gift from Dr. Matthew Rasband (Baylor College of Medicine; titer: 1×10^{13} GC/ml). In each case, 1–2 μl of solution containing each virus was injected into the locust right eye by use of a glass pipette as described above. Other procedures were as for the SFV vector.

Electrophysiology. The dissection of the locust optic lobe and electrophysiological procedures were described in previous papers (Dewell and Gabbiani 2018; Gabbiani et al. 2002; Wang et al. 2018). Initially, spikes of the descending contralateral movement detector (DCMD) neuron were recorded extracellularly by positioning hook electrodes around the ventral nerve cord. The signal was differentially amplified (gain: 10k; A-M Systems 1700, Sequim, WA) and monitored on an oscilloscope after additional amplification as needed (Neurophase 440, Palo Alto, CA). DCMD spikes were monitored to identify the LGMD in the lobula (Fig. 1B), since they are in one-to-one correspondence with LGMD spikes (O'Shea and Williams 1974). Sharp electrodes (~ 10 – 20 M Ω) were used for intracellular recording from the LGMD. The intracellular membrane potential was amplified using an intracellular amplifier (SEC-10 NPI, Tamm, Germany). Medullary neuronal activity was recorded extracellularly by using a pair of 5-M Ω tungsten electrodes (FHC, Bowdoin, ME). See Wang et al. (2018) for further details on electrophysiological methods.

Imaging using two-photon microscopy. The LGMD was stained with Alexa 594 injected iontophoretically through the sharp intracellular electrode (-1 nA alternating 1 s on and 1 s off current pulses; Dewell and Gabbiani 2018). The Venus-tagged presynaptic neurons, especially their axon terminals, and the LGMD were visualized using two-photon microscopy. The custom two-photon microscope used is described in Zhu and Gabbiani (2018). The excitation wavelength was set at 830 nm for Alexa 594 and 920 nm for Venus. Pictures were taken at successive depths separated by 1 μm . The images in Fig. 1 are mean projections of multiple frames. Figure 1, C and D, were averaged over 10 and 20 successive frames. Figure 1, E and F, are merged images from two channels, with the green channel (Venus) averaged over ~ 10 successive frames. The red channel (Alexa 594) was averaged over a larger depth to show the LGMD morphology.

Optogenetic stimulation. A 488-nm cyan laser with maximum output of 20 mW was used to stimulate ChopWR-expressing neurons in the optic lobe (model no. PC13589; Newport, Ottawa, ON, Can-

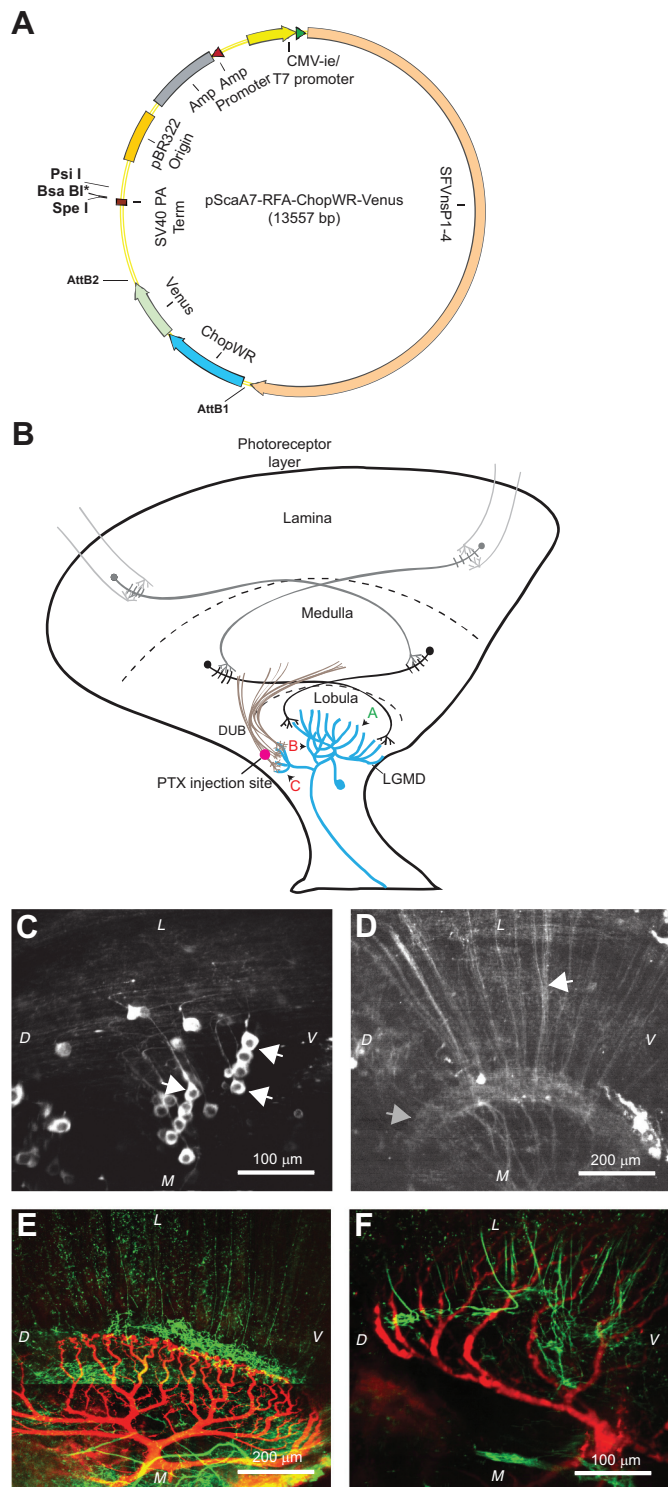


Fig. 1. Semliki Forest Virus (SFV) drives Chop-wide receiver (ChopWR)-Venus expression in medullary neurons of the locust optic lobe. **A**: schematic diagram showing the plasmid used to generate SFV A7(74)-based vectors encoding ChopWR-Venus. The viral backbone is derived from pSFV(A774nsP) (Ehrengruber et al. 2003). **B**: schematic of the locust visual system, showing the location of the lobula giant movement detector (LGMD) in the lobula neuropil of the optic lobe. Its 3 dendritic fields (A–C) are labeled in red. Picrotoxin (PTX) was injected in the dorsal uncrossed bundle (DUB) that mediates inhibition to field C. **C**: medullary neuron somata expressed ChopWR-Venus in the locust optic lobe (white arrows). **D**: bundles of transmedullary axons expressing ChopWR-Venus (white arrow) travel toward the lobula neuropil (gray arrow). **E** and **F**: double stain of the LGMD excitatory dendritic field (Alexa 594, red) and Venus-labeled transmedullary neuron terminal arbors (green) show close apposition in the lobula. **E** shows the general structure of the afferents contacting the excitatory dendritic field of the LGMD. **F** is a close-up showing the organization of afferent axons and presynaptic terminals in the immediate vicinity of dendritic field A. L, lateral; M, medial; D, dorsal; V, ventral. Scale bars are listed in each panel. C–F are from 4 different animals.

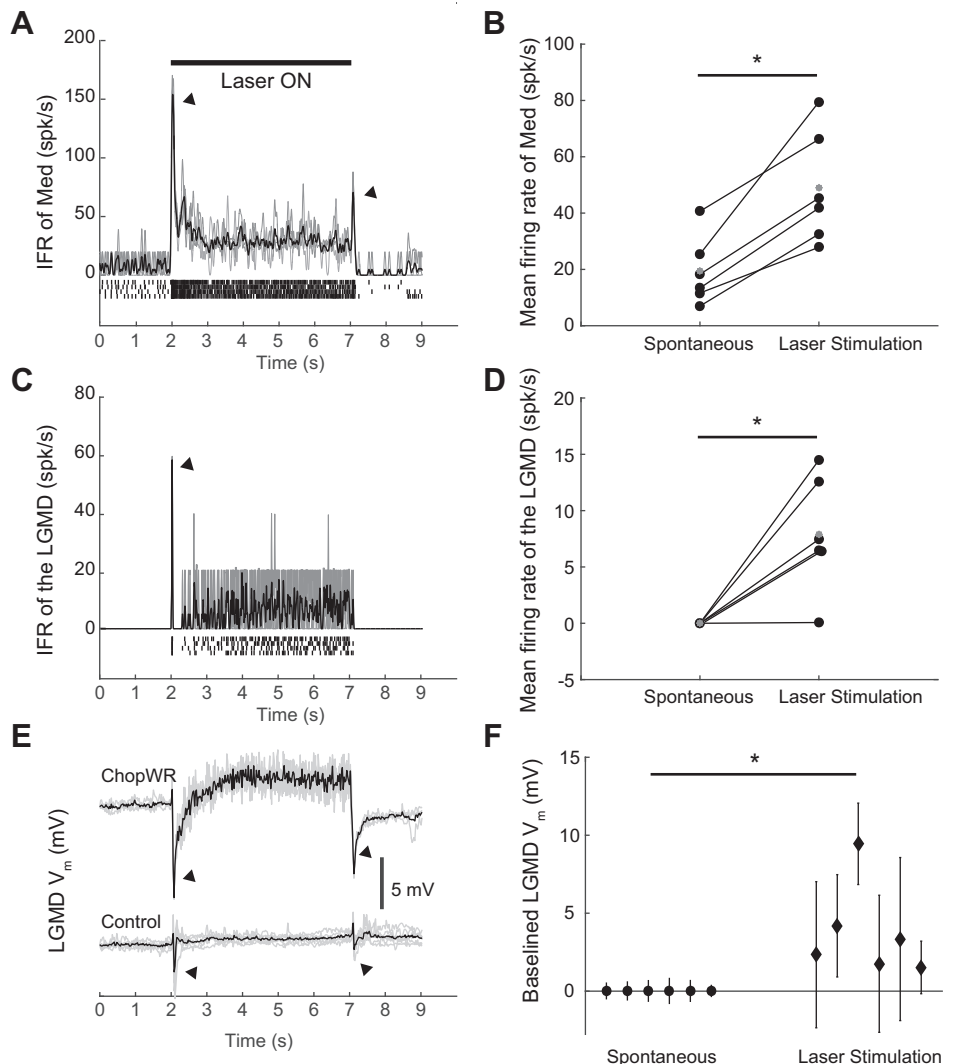
ada). Optic fibers (Thorlabs, Newton, NJ) with diameters of 10, 25, and 200 μm were used to deliver laser light. The optic fiber was connected to the 488-nm cyan laser via a collimator (F240FC-A, Thorlabs). The area of the incident laser beam arriving at the optic lobe was $\sim 1 \text{ mm}^2$. The laser power was varied between 2 and 20 mW by inserting neutral density filters at the output port of the laser, immediately before the collimator, with transmission rates of 10, 25, 40, 63, and 79%, respectively. To restrict the number of activated neurons, a custom-designed laser probe yielding a laser beam with a diameter of $\sim 10 \mu\text{m}$ was used in a subset of experiments (Segev et al. 2017). The time interval between two successive laser stimulations was 2 min to minimize desensitization of the responses. To minimize photoreceptor activation from reflected laser light, the eye was covered with black wax and/or black vinyl tape during laser stimulation. Despite this precaution, light hitting the back of the eye caused small, transient photoreceptor activations when the laser switched on and off.

Injection of picrotoxin in the lobula. To investigate whether inhibitory neurons presynaptic to the LGMD had been activated by the laser stimulation, picrotoxin (5 mM; Sigma-Aldrich, St. Louis, MO) dissolved in water was puffed along the dorsal edge of the lobula, close to the region where the inhibitory dendrites of the LGMD's fields B and C arborize (Fig. 1B). The injected solution contained 0.5% of the colorant fast green (Sigma-Aldrich) to visualize the tip of the injection pipette and the amount of solution injected into the lobula. The injection pipette's tip diameter varied between 1 and 2.5 μm . After injection, the dye diffused around the injection site and

stayed confined to the lobula. A picospritzer was used to control the duration and puffing pressure (8 psi/55 kPa; WPI). Based on earlier work (Dewell and Gabbiani 2018), the estimated final concentration of drug at the level of field C was $\leq 200 \mu\text{M}$.

Data analysis and statistics. Custom Matlab code was used for data analysis (The MathWorks, Natick, MA). The raw data recorded from medullary neurons were first normalized; the spikes were then detected with a set threshold (see Wang et al. 2018 for details). Spikes within 1.5 ms of a previously detected spike were excluded. To calculate instantaneous firing rates (IFRs) during looming stimuli, the spike train of the LGMD and the medullary neurons were convolved with a Gaussian filter that had a standard deviation of 20 ms. In Fig. 2E, the membrane potential (V_m) of the LGMD was median filtered over a time window of 25 ms to eliminate spikes and reveal the subthreshold V_m time course. For the same reason, in Fig. 2F the average LGMD's V_m during laser stimulation was calculated as its median value during the time interval when the laser was on. It was compared with the LGMD's V_m during spontaneous activity, calculated as the median value during the time interval from the start of recording to the start of laser stimulation ($>1 \text{ s}$). Medians for each trial were then averaged across three to five trials per animal. The mean firing rates shown in Fig. 3, D and E, were calculated during the 0.25-s periods after laser onset and offset, respectively. In Fig. 3C, the mean firing rate for the laser response was calculated from 0.25 s after its onset until 0.1 s before its offset. When the custom laser probe was being used, no spiking was evoked, and the LGMD's V_m

Fig. 2. Laser stimulation via optic fiber with a diameter of 200 μm activated the medullary neurons (Med) expressing Chop-wide receiver (ChopWR)-Venus and the lobula giant movement detector (LGMD). **A:** instantaneous firing rate of medullary neurons expressing ChopWR-Venus was increased during 5 s of 488-nm laser stimulation; *top*: laser stimulation timing; *bottom*, black trace is the averaged firing rate across 4 trials (gray traces). Rasters below the instantaneous firing rate (IFR) show the medullary neuronal spikes. **B:** mean firing rate (gray symbols) of the medullary neurons expressing ChopWR-Venus across 6 locusts (connected black dots) was compared with and without laser stimulation; $*P = 0.0156$ (one-sided Wilcoxon signed rank test). **C:** instantaneous firing rate of the LGMD increased during 5 s of 488-nm laser stimulation; black trace is the averaged firing rate across 4 trials (gray traces). Rasters below the IFR show the LGMD spikes. **D:** mean firing rate of the LGMD across 6 locusts (black dots) was compared with and without laser stimulation; $*P = 0.0156$. **E:** LGMD membrane potential (V_m) was depolarized during 5 s of 488-nm laser stimulation in a ChopWR-expressing locust (*top*), whereas no depolarization was observed in an untransfected control (*bottom*). Black trace represents the averaged V_m ; gray traces are individual trials (4 trials in the ChopWR-expressing locust and 6 trials in the wild-type locust). **F:** plot of mean median LGMD V_m ($\pm 1 \text{ SD}$) with and without laser stimulation in 6 animals. $*P = 0.0156$.



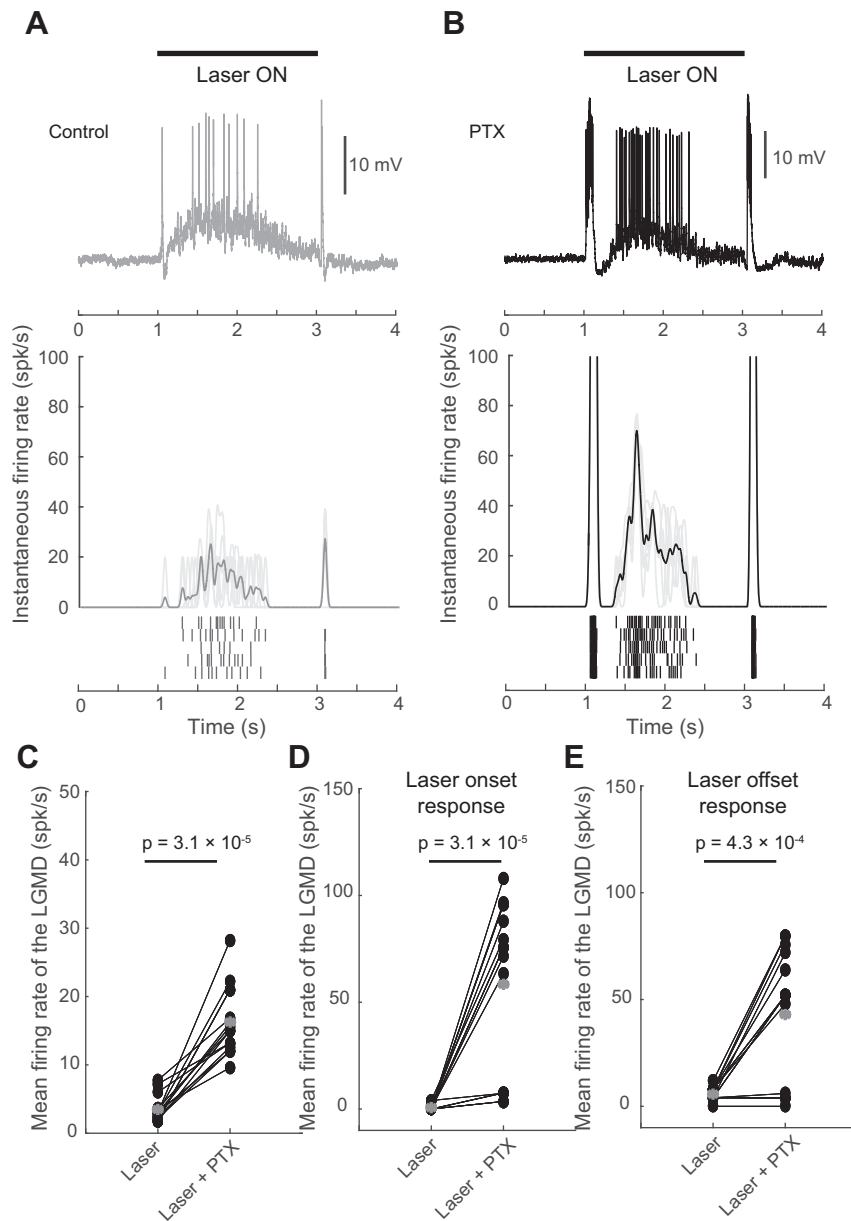


Fig. 3. Laser stimulation triggers inhibitory inputs to the lobula giant movement detector (LGMD) that can be blocked by the γ -aminobutyric acid A ($GABA_A$) receptor antagonist picrotoxin (PTX, $\leq 200 \mu\text{M}$; see MATERIALS AND METHODS). *A*: laser stimulation (2 s, 488 nm) via an optic fiber with diameter of $10 \mu\text{m}$ triggered the firing of the LGMD. *Top*: laser stimulation timing; *middle*: LGMD membrane potential (V_m) from 1 trial; *bottom*: the averaged LGMD instantaneous firing rate (IFR; gray trace) across 5 trials (light gray traces). Rasters below are spikes of the LGMD from 5 trials. *B*: puffing PTX increased laser-triggered firing in the LGMD. *Top*: laser stimulation timing; *middle*: LGMD V_m from 1 trial; *bottom*: averaged LGMD IFR (black trace) across 5 trials (light gray traces). Rasters below are spikes of the LGMD from 5 trials. *C*: firing rate of the LGMD triggered by laser stimulation from 15 trials in 3 locusts (5 per animal) was compared with and without puffing PTX [$P = 3.1 \times 10^{-5}$, one-sided Wilcoxon signed rank test (WRST)]. *D* and *E*: mean firing rates of the LGMD triggered by laser onset (*D*) and offset (*E*) from 15 trials in 3 locusts were compared with and without puffing PTX ($P = 3.1 \times 10^{-5}$ and 4.3×10^{-4} , one-sided WRST). Gray symbols indicate mean values across 15 trials in 3 locusts. Connected black dots are single trials.

during laser stimulation was calculated as the mean of the V_m during the time when the laser was on (see Fig. 5B). It was compared with the LGMD's V_m during spontaneous activity, calculated as the mean within 1 s before the start of laser stimulation (see Fig. 5C).

The one-sided Wilcoxon signed rank test (WSRT) was used to compare the statistical differences between groups of spontaneous activities and activities stimulated by optogenetics with or without picrotoxin treatment. All the data are described as means \pm SD.

RESULTS

SFV drives expression of ChopWR-Venus in locust medullary neurons. In pilot experiments, we tested with little success the capacity of several viruses to transfect locust optic lobe neurons, including AAV, Sindbis, and baculovirus. Although AAV is not known to infect arthropods, other members of its family as well as Sindbis and baculovirus do (Cotmore et al. 2014; Lewis et al. 1999; Oppenheimer et al. 1999). In contrast,

3 days after recombinant SFV injection, ChopWR-Venus was observed expressing on the membrane of medullary neuron cell bodies, axonal fibers, and presynaptic terminals in the lobula (Fig. 1, C–F). When the LGMD was concurrently stained with the fluorescent dye Alexa 594, some axon terminals overlapped with the dendritic branches of the LGMD (Fig. 1, E and F). Additionally, stained neurons were also observed in the lamina in some experiments, when viral solution was deposited there upon retraction of the injection pipette (not shown). These results indicate that the SFV A7(74) plasmid vector can efficiently deliver a gene of interest into neurons of the medulla (and lamina) of the locust optic lobe. In addition to optic lobe neurons, we also observed ChopWR-Venus-stained neurons in the brain and the subesophageal ganglion in some experiments. Five of 70 animals injected with virus died; all other locusts were healthy and did not appear to be affected negatively by the manipulation during the experiments.

Optogenetic stimulation of medullary neurons activates the LGMD. As demonstrated in Fig. 2A, the instantaneous firing rate (IFR) of transfected medullary neurons increased in response to a 5-s-long laser pulse. On average, the spontaneous firing rate of medullary units recorded from a pair of tungsten electrodes was 19.4 ± 12.2 spk/s (mean \pm SD), while optogenetic stimulation increased the rate to 48.9 ± 20.0 spk/s (Fig. 2B). The IFR of the LGMD increased as well (Fig. 2C). On average, the mean firing rate of the LGMD in response to laser stimulation increased from 0 to 7.9 ± 5.1 spk/s (Fig. 2D). The turning on and off of the laser caused brief spike bursts in the medullary neurons (Fig. 2A, arrowheads). Correspondingly, the LGMD fired an initial spike right after the on transition (Fig. 2C, arrowhead), which was immediately followed by a transient membrane potential (V_m) hyperpolarization of ~ 1 s duration, also observed right after the laser was turned off (Fig. 2E, top, arrowheads). During the laser stimulation, the LGMD V_m was depolarized by 3.8 ± 3.0 mV (Fig. 2, E and F) in the ChopWR-expressing locusts. As the LGMD receives excitatory inputs through cholinergic synapses on dendritic field A (Fig. 1B), such depolarizations result from compound excitatory postsynaptic potentials (EPSPs) originating from ChopWR-stimulated medullary presynaptic afferents (Peron et al. 2009; Zhu et al. 2018). Individual EPSPs elicited by laser stimulation are documented below (last subsection of RESULTS). In uninjected controls, transient responses occurred with laser onset and offset, but no sustained membrane potential depolarization was observed (Fig. 2E, bottom). These findings imply that optogenetic manipulation of medullary neurons is able to modulate the sub- and suprathreshold activity of one downstream target neuron, the LGMD.

Block of inhibition enhances LGMD firing to optogenetic stimulation. To isolate the excitatory inputs to the LGMD, the γ -aminobutyric acid A (GABA_A) receptor antagonist picrotoxin was puffed at the dorsal edge of the lobula, where inhibitory dendritic branches of the LGMD are located (dendritic fields B and C; Fig. 1B). Compared with the control group, block of inhibition increased the firing of the LGMD in response to the laser stimulation (Fig. 3, A and B). The LGMD firing rate caused by the laser stimulation increased from 3.5 ± 1.9 to 16.2 ± 4.9 spk/s after adding picrotoxin ($P = 3.1 \times 10^{-5}$, one-sided WSRT; Fig. 3C). Addition of picrotoxin removed the hyperpolarizations observed at the onset and offset of the laser pulse (Fig. 2E). Instead, the luminance change caused by the laser turning on and off produced transient bursts with mean firing rates of 58.6 ± 40.2 and 43.0 ± 30.7 spk/s after GABA_A blockade ($P = 3.1 \times 10^{-5}$ and 4.3×10^{-4} , one-sided WSRT; Fig. 3, B, D, and E). These results demonstrated that the combination of blocker and optogenetic stimulation was largely effective at isolating the excitatory input to the LGMD.

Laser power affects the firing of the LGMD. Next, we tested whether optogenetic activation of the LGMD depends on the strength of the laser power stimulus used to activate channelrhodopsin. As demonstrated for one example in Fig. 4A, the mean number of spikes of the LGMD across five trials increased from 19.8 ± 3.3 to 44.6 ± 14.7 when power increased from 2 to 8 mW. However, at the higher power of 16 mW, the number of LGMD spikes elicited by the laser stimulus was slightly lower, 33.2 ± 11.9 . We further investigated the effect of laser power in five animals by using six values varying from

2 to 20 mW (Fig. 4B). As shown in Fig. 4B, we found that spiking increased when power was increased from 2 to 5 and 8 mW (18.4 ± 6.2 , 31.3 ± 19.1 and 37.7 ± 23.3 , respectively). However, higher powers of 13, 16, and 20 mW resulted in slightly decreased spiking output than at 8 mW (28.2 ± 19.0 , 28.4 ± 16.9 and 30.6 ± 17.4 , respectively). The decrement might have been caused by desensitization of channelrhodopsin at stronger laser power (Lin 2011; Wang et al. 2009). These results indicate that optogenetic activation of the LGMD can be modulated by the laser power strength for a given expression level of ChopWR in medullary neurons.

Narrow laser beam produces less LGMD activation. When we varied the diameter of the optic fibers used to deliver the stimulus to the optic lobe from 10 to 200 μ m, we found that the illuminated region did not change much, always being ~ 1 mm². To further spatially restrict the number of neurons activated by the laser stimulus, we replaced the optic fiber with a specialized custom laser probe with an exit beam diameter of 10 μ m (Fig. 5A; METHODS). As demonstrated in Fig. 5B, illumination transmitted by this laser probe triggered EPSPs but no spiking in the LGMD, except for the spikes evoked by the on and off stimulation caused by the laser light onset and offset. The average LGMD's V_m during laser probe illumination was significantly depolarized in the first 2 s (0.5 ± 0.3 mV) and over the whole duration of laser illumination (0.2 ± 0.3 mV). These results indicate that the modified laser probe is suitable for restricting the number of neurons activated by laser light.

DISCUSSION

In this study, we demonstrated that SFV A7(74) drove ChopWR-Venus expression on the cell membrane of medullary neurons in the locust optic lobe. Laser illumination increased the firing rate of the medullary neurons expressing ChopWR-Venus and triggered EPSPs and the firing of a downstream lobula neuron, the LGMD, which plays a key role in the locust visual collision detection circuit. SFV A7(74) mediated highly efficient expression of ChopWR-Venus and led to the labeling of many neurons in the region surrounding the injection site. These findings provide a way to express genes of interest in locust neurons and to modulate neuronal activity using optogenetics. Besides optogenetics, genetically encoded calcium indicators (Akerboom et al. 2012) are future candidates for expression in locust medullary neurons via SFV A7(74) transfection. These tools will help identify anatomically medullary neurons and study their roles in specific visual processing tasks through characterization of their calcium responses to different visual stimuli. In the specific context of the LGMD collision avoidance circuit, SFV transfection could be used to coexpress ChopWR and genetically encoded calcium indicators (as described in Ehrengreuer 2002), allowing to identify neurons presynaptic to the LGMD by localized optogenetic stimulation (Fig. 5), followed by Ca²⁺ imaging to study their activation in response to simulated objects approaching on a collision course. ChopWR-Venus-mediated expression could also be targeted to the DCMD neuron postsynaptic to the LGMD by injection into the brain proper (protocerebrum) rather than the optic lobe. This would allow stimulating the DCMD optically in a freely behaving animal to test the role of the LGMD and DCMD neurons in visually evoked jump escape behavior, extending the results of Fotowat

et al. (2011). More generally, because SFV infects neurons in a variety of species, including locusts, mosquitoes, *Drosophila*, ticks, and mammalian cells (Ehrengruber et al. 1999; Liljeström and Garoff 1991; Lwande et al. 2013; Wimmer et al. 2004), it is likely to be effective in other insect species, such as orthoptera closely related to *Schistocerca americana*.

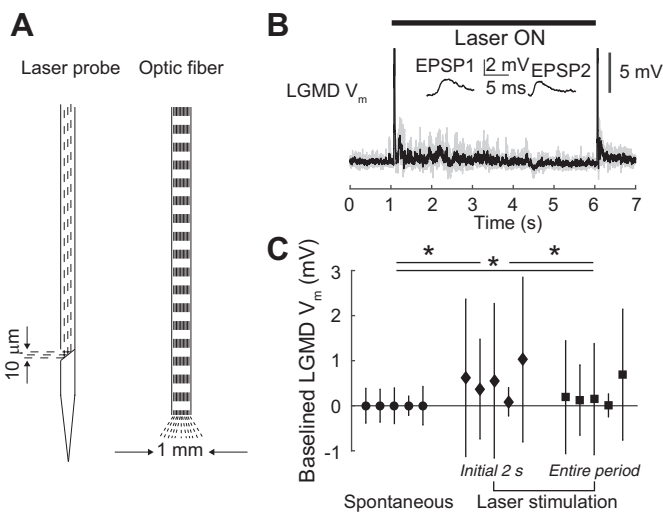
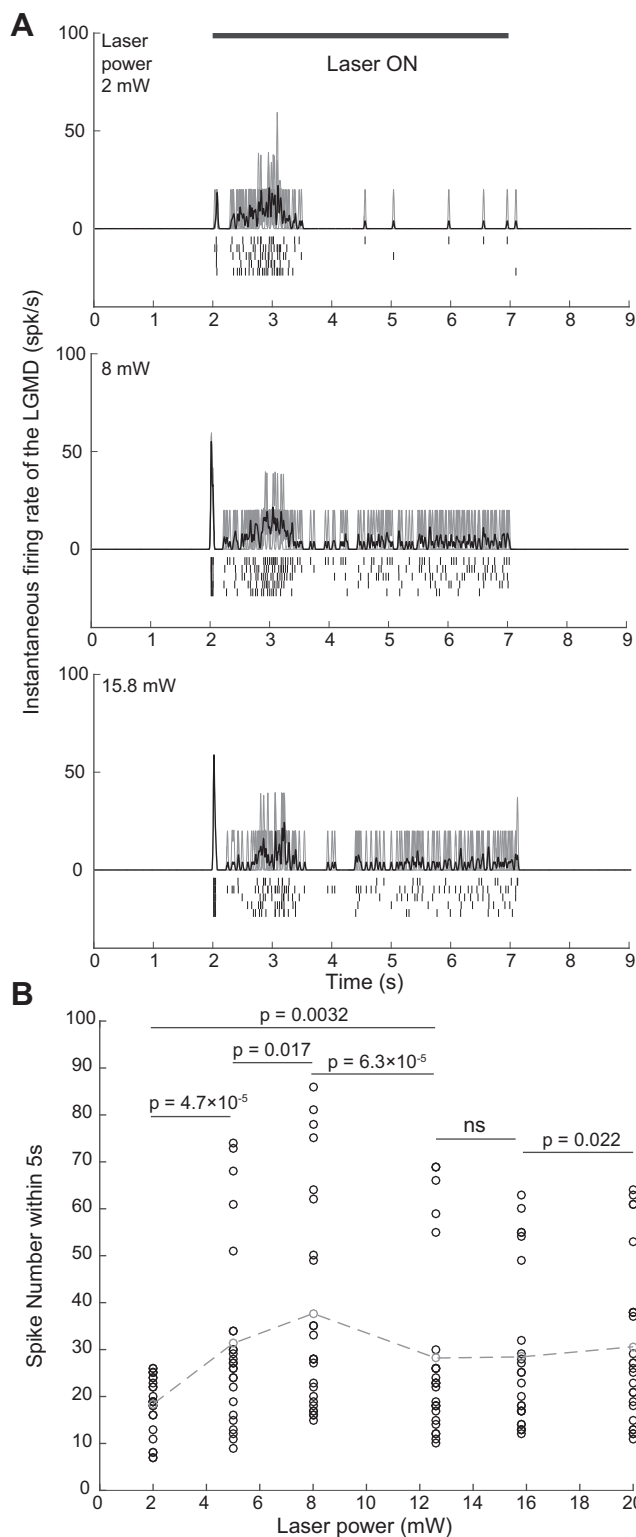


Fig. 5. A laser probe narrowing the region activated by the laser elicited only excitatory postsynaptic potentials (EPSPs) in the lobula giant movement detector (LGMD). **A**: schematics of the laser probe (*left*) and optic fiber (*right*). Dashed lines indicate light path. In the laser probe, the beam exits perpendicular to the shaft, thanks to a mirror. In the laser probe, the beam exits perpendicular to the shaft, thanks to a mirror. **B**: laser probe stimulation (5 s, 488 nm) triggered EPSPs in the LGMD. *Top*: laser stimulation timing; *bottom*: averaged LGMD membrane potential (V_m ; black trace) across 4 trials (gray traces). *Middle inset*: 2 examples of single EPSPs triggered by laser stimulation. **C**: comparison of the mean across 3–5 trials of the LGMD V_m (± 1 SD) for 5 locusts with and without laser stimulation. For each animal, mean V_m was higher during laser stimulation and higher during the first 2 s than the last 3 s of laser stimulation. $*P = 0.0312$ by one-sided Wilcoxon signed rank test.

The responses immediately after the laser onset and offsets (arrowheads in Fig. 2; initial spikes in Figs. 3 and 4) were likely caused, in part, by photoreceptor activation from scattered laser light hitting the back of the eye. In experiments without viral transfection, no prolonged change in LGMD activity occurred in response to laser stimulation (Fig. 2*E*, *bottom*). The prolonged activation of medullary neurons and the LGMD during laser illumination were not attributable to the activation of photoreceptors and therefore are believed to be solely due to the light-gated ChopWR current influx into these neurons.

Because the large number of medullary neurons expressing ChopWR-Venus contained a mixture of both excitatory and inhibitory neurons, it was hard to precisely control neuronal activation of the LGMD through optogenetic stimulation. The specificity of LGMD activation could be substantially increased by blocking inhibitory inputs to the LGMD pharmacologically (Fig. 3). Another way of getting more specific activation was by reducing the area of laser illumination. We

Fig. 4. Firing of the lobula giant movement detector (LGMD) increased and saturated in response to increasing laser power. **A**, Examples of the LGMD instantaneous firing rate (IFR) in response to laser powers of 2, 8, and 16 mW (from *top* to *bottom*; 1 locust). Laser stimulation timing is shown above the *top* panel (duration: 5 s). Each panel shows the averaged LGMD IFR (black) from 5 trials (gray traces). Rasters below the LGMD IFR are LGMD spikes from the 5 trials ($P = 0.0312$ and 0.125 between groups with laser power at 2 vs. 8, and 8 vs. 16 mW by a one-sided Wilcoxon signed rank test). **B**: number of LGMD spikes evoked by laser stimulation increased and saturated with increasing power. Gray circles connected by gray dashed line indicate mean value in each group. A Kruskal-Wallis test was used to evaluate the effect of laser power across groups ($P = 0.013$). A post hoc signed rank test was used to evaluate the difference between 2 groups (5 locusts, 25 trials for each laser power; P values are on panels; ns, no significant difference).

tested a specialized custom laser probe that minimizes the size of the laser beam and thus limits the number neurons activated (Fig. 5). In this configuration, only EPSPs but no spikes were evoked in the LGMD by optogenetic stimulation. However, a cell type-specific pattern of neural activation could not be achieved with currently available tools. In genetic model systems such as mice and fruit flies, there are ways to generate cell type-specific gene expression. In mice, for example, the Cre-LoxP system drives cell type-specific expression through defined promoters (Sauer 1998). The Gal4-UAS system is one of the most powerful ways of achieving targeted gene expression in *Drosophila* that has been adapted to other model systems (Asakawa and Kawakami 2008; Brand and Perrimon 1993; Busson and Pret 2007; Imamura et al. 2003). This binary system is widely used to create transgenic flies by combining a driver (Gal4) and responder (UAS) line based on the properties of the yeast transcription factor Gal4, which activates its target genes by binding to UAS *cis*-regulatory sites. For transient gene expression in locusts, it would also be desirable to target genes to specific cell types. However, this is not yet feasible due to a lack of identification of cell type-specific promoters and of transgenic locust lines expressing an effector gene under their control.

Yet, other possibilities to target gene expression in specific cell types exist. MicroRNAs (miRNAs) are small noncoding RNAs involved in posttranscriptional regulation of gene expression (Obernosterer et al. 2006). Recently, miRNAs have been applied to detarget gene expression when a SFV-derived oncolytic virus is used to treat tumors such as glioblastoma (Ramachandran et al. 2017; Ylösmäki et al. 2013). The working principle of miRNAs is that by integrating the complementary sequence of a miRNA into the viral genome downstream of the viral subgenomic promoter, the miRNAs expressed in specific cells can identify the complementary sequence and cause the degradation of viral mRNA. This in turn reduces the expression of viral proteins in those cells. Wild-type SFV is naturally neurotropic (e.g., Ehrenguber et al. 1999). So, to protect neurons from SFV-based cancer virotherapy, the neuron-specific miRNAs miR124, miR125, and miR134 were inserted into the SFV4 vector genome. This resulted in attenuated neurovirulence in cultured neurons, astrocytes, and oligodendrocytes, and it also attenuated neurovirulence in adult mice, but the modified virus retained its replication ability in murine neural stem cells, where the expression of these miRNAs is low (Ramachandran et al. 2017; Ylösmäki et al. 2013).

Interestingly, abundant miRNAs have been identified in tissues of a species closely related to that studied here, *Locusta migratoria*, including the pronotum, testes, antennae, fat bodies, and brain (Wang et al. 2015). Homology searches indicated that tissue-specific miRNAs were also lineage specific and that many of them were specifically expressed in the brain. Thus, provided information becomes available in the future on the expression pattern of the miRNAs in specific cell populations, such as excitatory or inhibitory neurons, one could add their complementary sequence to SFV plasmids and obtain specific gene expression in the locust.

Injecting a viral vector containing a gene of interest in insects will produce only transient expression. Creating a transgenic line would be optimal to get stable foreign gene expression. Transgenic houseflies (Hediger et al. 2001), silkworms (Tamura et al. 2000), ants (Trible et al. 2017), honey-

bees (Schulte et al. 2014), and crickets (Nakamura et al. 2010) have been created using a transposon *piggyBac*-derived vector. CRISPR/Cas9 has been successfully used to generate stable transgenic germlines in *Drosophila*, mosquitoes, and locusts (Bassett et al. 2013; Kistler et al. 2015; Li et al. 2016). In the locust, one recently identified miRNA precursor is likely a transposable element from a long-interspersed element family (Wang et al. 2015). One could thus try this putative locust-specific transposable element or use the transposon *piggyBac*-derived vector described by Nakamura et al. (2010) or alternatively use CRISPR/Cas9 technology to generate additional stable transgenic germline transformations (Li et al. 2016).

ACKNOWLEDGMENTS

We thank Drs. Hiromu Yawo and Toru Ishizuka for providing pChopWR-Venus. We also thank Drs. Emma Victoria Jones and Keith Murai for providing the plasmids pENTR2B and pScaA7-RFA, and Dr. Alan L. Goldin for the pSFV-Helper2.

GRANTS

This work was supported by a grant from the National Institute of Mental Health (MH-065339) and the National Science Foundation (IIS-1607518).

DISCLOSURES

No conflicts of interest, financial or otherwise, are declared by the authors.

AUTHOR CONTRIBUTIONS

H.W., M.U.E., J.R., M.L.R., and F.G. conceived and designed research; H.W., R.B.D., E.S., and J.R. performed experiments; H.W. and R.B.D. analyzed data; H.W., R.B.D., and F.G. interpreted results of experiments; H.W. and F.G. prepared figures; H.W. and F.G. drafted manuscript; H.W., R.B.D., M.U.E., and F.G. edited and revised manuscript; H.W., R.B.D., M.U.E., E.S., J.R., M.L.R., and F.G. approved final version of manuscript.

REFERENCES

- Adamantidis AR, Zhang F, Aravanis AM, Deisseroth K, de Lecea L. Neural substrates of awakening probed with optogenetic control of hypocretin neurons. *Nature* 450: 420–424, 2007. doi:10.1038/nature06310.
- Akerboom J, Chen T-W, Wardill TJ, Tian L, Marvin JS, Mutlu S, Calderón NC, Esposti F, Borghuis BG, Sun XR, Gordus A, Orger MB, Portugues R, Engert F, Macklin JJ, Filosa A, Aggarwal A, Kerr RA, Takagi R, Kracun S, Shigetomi E, Khakh BS, Baier H, Lagnado L, Wang SS, Bargmann CI, Kimmel BE, Jayaraman V, Svoboda K, Kim DS, Schreiter ER, Looger LL. Optimization of a GCaMP calcium indicator for neural activity imaging. *J Neurosci* 32: 13819–13840, 2012. doi:10.1523/JNEUROSCI.2601-12.2012.
- Arenkiel BR, Peca J, Davison IG, Feliciano C, Deisseroth K, Augustine GJ, Ehlers MD, Feng G. In vivo light-induced activation of neural circuitry in transgenic mice expressing channelrhodopsin-2. *Neuron* 54: 205–218, 2007. doi:10.1016/j.neuron.2007.03.005.
- Arrenberg AB, Del Bene F, Baier H. Optical control of zebrafish behavior with halorhodopsin. *Proc Natl Acad Sci USA* 106: 17968–17973, 2009. doi:10.1073/pnas.0906252106.
- Asakawa K, Kawakami K. Targeted gene expression by the Gal4-UAS system in zebrafish. *Dev Growth Differ* 50: 391–399, 2008. doi:10.1111/j.1440-169X.2008.01044.x.
- Bassett AR, Tibbit C, Ponting CP, Liu J-L. Highly efficient targeted mutagenesis of *Drosophila* with the CRISPR/Cas9 system. *Cell Reports* 4: 220–228, 2013. [Erratum in *Cell Reports* 6: P1178–P1179, 2014.] doi:10.1016/j.celrep.2013.06.020.
- Berglund P, Sjöberg M, Garoff H, Atkins GJ, Sheahan BJ, Liljeström P. Semliki Forest virus expression system: production of conditionally infectious recombinant particles. *Biotechnology (N Y)* 11: 916–920, 1993.
- Bi A, Cui J, Ma Y-P, Olshevskaya E, Pu M, Dizhoor AM, Pan Z-H. Ectopic expression of a microbial-type rhodopsin restores visual responses in mice

- with photoreceptor degeneration. *Neuron* 50: 23–33, 2006. doi:10.1016/j.neuron.2006.02.026.
- Boyd ES, Zhang F, Bamberg E, Nagel G, Deisseroth K. Millisecond-timescale, genetically targeted optical control of neural activity. *Nat Neurosci* 8: 1263–1268, 2005. doi:10.1038/nn1525.
- Brand AH, Perrimon N. Targeted gene expression as a means of altering cell fates and generating dominant phenotypes. *Development* 118: 401–415, 1993.
- Busson D, Pret A-M. GAL4/UAS targeted gene expression for studying drosophila hedgehog signaling. In: *Hedgehog Signaling Protocols*, edited by Horabin JI. Totowa, NJ: Humana, 2007, p. 161–201.
- Cotmore SF, Agbandje-McKenna M, Chiorini JA, Mukha DV, Pintel DJ, Qiu J, Soderlund-Venermo M, Tattersall P, Tijssen P, Gatherer D, Davidson AJ. The family *Parvoviridae*. *Arch Virol* 159: 1239–1247, 2014. doi:10.1007/s00705-013-1914-1.
- Dewell RB, Gabbiani F. Biophysics of object segmentation in a collision-detecting neuron. *eLife* 7: e34238, 2018. doi:10.7554/eLife.34238.
- DiCiommo DP, Bremner R. Rapid, high level protein production using DNA-based Semliki Forest virus vectors. *J Biol Chem* 273: 18060–18066, 1998. doi:10.1074/jbc.273.29.18060.
- Egelhaaf M. Fly vision: neural mechanisms of motion computation. *Curr Biol* 18: R339–R341, 2008. doi:10.1016/j.cub.2008.02.046.
- Ehrengruber MU. Alphaviral gene transfer in neurobiology. *Brain Res Bull* 59: 13–22, 2002. doi:10.1016/S0361-9230(02)00858-4.
- Ehrengruber MU, Lundstrom K, Schweitzer C, Heuss C, Schlesinger S, Gähwiler BH. Recombinant Semliki Forest virus and Sindbis virus efficiently infect neurons in hippocampal slice cultures. *Proc Natl Acad Sci USA* 96: 7041–7046, 1999. doi:10.1073/pnas.96.12.7041.
- Ehrengruber MU, Renggli M, Raineteau O, Hennou S, Vähä-Koskela MJV, Hinkkanen AE, Lundstrom K. Semliki Forest virus A7(74) transduces hippocampal neurons and glial cells in a temperature-dependent dual manner. *J Neurovirol* 9: 16–28, 2003. doi:10.1080/13550280390173346.
- Ehrengruber MU, Schlesinger S, Lundstrom K. Alphaviruses: Semliki Forest virus and Sindbis virus vectors for gene transfer into neurons. *Curr Protocols Neurosci* 57: 4.22.1–4.22.27, 2011.
- Evangelista C, Kraft P, Dacke M, Labhart T, Srinivasan MV. Honeybee navigation: critically examining the role of the polarization compass. *Philos Trans R Soc Lond B Biol Sci* 369: 20130037, 2014. doi:10.1098/rstb.2013.0037.
- Fotowat H, Gabbiani F. Collision detection as a model for sensory-motor integration. *Annu Rev Neurosci* 34: 1–19, 2011. doi:10.1146/annurev-neuro-061010-113632.
- Fotowat H, Harrison RR, Gabbiani F. Multiplexing of motor information in the discharge of a collision detecting neuron during escape behaviors. *Neuron* 69: 147–158, 2011. doi:10.1016/j.neuron.2010.12.007.
- Gabbiani F, Krapp HG, Koch C, Laurent G. Multiplicative computation in a visual neuron sensitive to looming. *Nature* 420: 320–324, 2002. doi:10.1038/nature01190.
- Göpfert MC, Hennig RM. Hearing in insects. *Annu Rev Entomol* 61: 257–276, 2016. doi:10.1146/annurev-ento-010715-023631.
- Gradinaru V, Mogri M, Thompson KR, Henderson JM, Deisseroth K. Optical deconstruction of parkinsonian neural circuitry. *Science* 324: 354–359, 2009. doi:10.1126/science.1167093.
- Gupta N, Stopfer M. Insect olfactory coding and memory at multiple timescales. *Curr Opin Neurobiol* 21: 768–773, 2011. doi:10.1016/j.conb.2011.05.005.
- Hales KG, Korey CA, Larracuenta AM, Roberts DM. Genetics on the fly: a primer on the *Drosophila* model system. *Genetics* 201: 815–842, 2015. doi:10.1534/genetics.115.183392.
- Hediger M, Niessen M, Wimmer EA, Dübendorfer A, Bopp D. Genetic transformation of the housefly *Musca domestica* with the lepidopteran derived transposon piggyBac. *Insect Mol Biol* 10: 113–119, 2001. doi:10.1046/j.1365-2583.2001.00243.x.
- Imamura M, Nakai J, Inoue S, Quan GX, Kanda T, Tamura T. Targeted gene expression using the GAL4/UAS system in the silkworm *Bombyx mori*. *Genetics* 165: 1329–1340, 2003.
- Ishizuka T, Kakuda M, Araki R, Yawo H. Kinetic evaluation of photosensitivity in genetically engineered neurons expressing green algae light-gated channels. *Neurosci Res* 54: 85–94, 2006. doi:10.1016/j.neures.2005.10.009.
- Kistler KE, Voshall LB, Matthews BJ. Genome engineering with CRISPR-Cas9 in the mosquito *Aedes aegypti*. *Cell Reports* 11: 51–60, 2015. doi:10.1016/j.celrep.2015.03.009.
- Kohatsu S, Yamamoto D. Visually induced initiation of *Drosophila* innate courtship-like following pursuit is mediated by central excitatory state. *Nat Commun* 6: 6457, 2015. doi:10.1038/ncomms7457.
- Lewis DL, DeCamillis MA, Brunetti CR, Halder G, Kassner VA, Selegue JE, Higgs S, Carroll SB. Ectopic gene expression and homeotic transformations in arthropods using recombinant Sindbis viruses. *Curr Biol* 9: 1279–1287, 1999. doi:10.1016/S0960-9822(00)80049-4.
- Li Y, Zhang J, Chen D, Yang P, Jiang F, Wang X, Kang L. CRISPR/Cas9 in locusts: Successful establishment of an olfactory deficiency line by targeting the mutagenesis of an odorant receptor co-receptor (Orco). *Insect Biochem Mol Biol* 79: 27–35, 2016. doi:10.1016/j.ibmb.2016.10.003.
- Liljeström P, Garoff H. A new generation of animal cell expression vectors based on the Semliki Forest virus replicon. *Biotechnology (N Y)* 9: 1356–1361, 1991. doi:10.1038/nbt1291-1356.
- Lin JY. A user's guide to channelrhodopsin variants: features, limitations and future developments. *Exp Physiol* 96: 19–25, 2011. doi:10.1113/expphysiol.2009.051961.
- Lundstrom K, Abenavoli A, Malgaroli A, Ehrengruber MU. Novel Semliki Forest virus vectors with reduced cytotoxicity and temperature sensitivity for long-term enhancement of transgene expression. *Mol Ther* 7: 202–209, 2003. doi:10.1016/S1525-0016(02)00056-4.
- Lwande OW, Lutomiah J, Obanda V, Kakuya F, Mutisya J, Mulwa F, Michuki G, Chepkorir E, Fischer A, Venter M, Sang R. Isolation of tick- and mosquito-borne arboviruses from ticks sampled from livestock and wild animal hosts in Ijara District, Kenya. *Vector Borne Zoonotic Dis* 13: 637–642, 2013. doi:10.1089/vbz.2012.1190.
- Nagel G, Szellas T, Huhn W, Kateriya S, Adeishvili N, Berthold P, Ollig D, Hegemann P, Bamberg E. Channelrhodopsin-2, a directly light-gated cation-selective membrane channel. *Proc Natl Acad Sci USA* 100: 13940–13945, 2003. doi:10.1073/pnas.1936192100.
- Nakamura T, Yoshizaki M, Ogawa S, Okamoto H, Shinmyo Y, Bando T, Ohuchi H, Noji S, Mito T. Imaging of transgenic cricket embryos reveals cell movements consistent with a syncytial patterning mechanism. *Curr Biol* 20: 1641–1647, 2010. doi:10.1016/j.cub.2010.07.044.
- O'Shea M, Williams JLD. The anatomy and output connection of a locust visual interneurone; the lobular giant movement detector (LGMD) neurone. *J Comp Physiol A Neuroethol Sens Neural Behav Physiol* 91: 257–266, 1974. doi:10.1007/BF00698057.
- Obernosterer G, Leuschner PJF, Alenius M, Martinez J. Post-transcriptional regulation of microRNA expression. *RNA* 12: 1161–1167, 2006. doi:10.1261/rna.2322506.
- Oppenheimer DI, MacNicol AM, Patel NH. Functional conservation of the wingless-engrailed interaction as shown by a widely applicable baculovirus misexpression system. *Curr Biol* 9: 1288–1296, 1999. doi:10.1016/S0960-9822(00)80050-0.
- Peron SP, Jones PW, Gabbiani F. Precise subcellular input retinotopy and its computational consequences in an identified visual interneuron. *Neuron* 63: 830–842, 2009. doi:10.1016/j.neuron.2009.09.010.
- Ramachandran M, Yu D, Dyczynski M, Baskaran S, Zhang L, Lulla A, Lulla V, Saul S, Nelander S, Dimberg A, Merits A, Leja-Jarblad J, Essand M. Safe and effective treatment of experimental neuroblastoma and glioblastoma using systemically delivered triple microRNA-detargeted oncolytic Semliki Forest virus. *Clin Cancer Res* 23: 1519–1530, 2017. doi:10.1158/1078-0432.CCR-16-0925.
- Sauer B. Inducible gene targeting in mice using the Cre/lox system. *Methods* 14: 381–392, 1998. doi:10.1006/meth.1998.0593.
- Schlesinger S. Alphaviruses—vectors for the expression of heterologous genes. *Trends Biotechnol* 11: 18–22, 1993. doi:10.1016/0167-7799(93)90070-P.
- Schulte C, Theilenberg E, Müller-Borg M, Gempe T, Beyre M. Highly efficient integration and expression of piggyBac-derived cassettes in the honeybee (*Apis mellifera*). *Proc Natl Acad Sci USA* 111: 9003–9008, 2014. doi:10.1073/pnas.1402341111.
- Segev E, Reimer J, Moreaux LC, Fowler TM, Chi D, Sacher WD, Lo M, Deisseroth K, Tolia AS, Faraon A, Roukes ML. Patterned photostimulation via visible-wavelength photonic probes for deep brain optogenetics. *Neurophotonics* 4: 011002, 2017. doi:10.1117/1.NPh.4.1.011002.
- Spindler SR, Hartenstein V. The *Drosophila* neural lineages: a model system to study brain development and circuitry. *Dev Genes Evol* 220: 1–10, 2010. doi:10.1007/s00427-010-0323-7.
- Srinivasan MV. Honey bees as a model for vision, perception, and cognition. *Annu Rev Entomol* 55: 267–284, 2010. doi:10.1146/annurev.ento.010908.164537.

- Strauss JH, Strauss EG.** The alphaviruses: gene expression, replication, and evolution. *Microbiol Rev* 58: 491–562, 1994.
- Tamura T, Thibert C, Royer C, Kanda T, Eappen A, Kamba M, Kômoto N, Thomas J-L, Mauchamp B, Chavancy G, Shirk P, Fraser M, Prudhomme JC, Couble P.** Germline transformation of the silkworm *Bombyx mori* L. using a piggyBac transposon-derived vector. *Nat Biotechnol* 18: 81–84, 2000. [Erratum in *Nat Biotechnol* 18: 559, 2000.] doi:10.1038/71978.
- Trible W, Olivos-Cisneros L, McKenzie SK, Saragosti J, Chang N-C, Matthews BJ, Oxley PR, Kronauer DJC.** orco mutagenesis causes loss of antennal lobe glomeruli and impaired social behavior in ants. *Cell* 170: 727–735.e10, 2017. doi:10.1016/j.cell.2017.07.001.
- Umeda K, Shoji W, Sakai S, Muto A, Kawakami K, Ishizuka T, Yawo H.** Targeted expression of a chimeric channelrhodopsin in zebrafish under regulation of Gal4-UAS system. *Neurosci Res* 75: 69–75, 2013. doi:10.1016/j.neures.2012.08.010.
- Wang H, Dewell RB, Zhu Y, Gabbiani F.** Feedforward inhibition conveys time-varying stimulus information in a collision detection circuit. *Curr Biol* 28: 1509–1521.e3, 2018. doi:10.1016/j.cub.2018.04.007.
- Wang H, Sugiyama Y, Hikima T, Sugano E, Tomita H, Takahashi T, Ishizuka T, Yawo H.** Molecular determinants differentiating photocurrent properties of two channelrhodopsins from chlamydomonas. *J Biol Chem* 284: 5685–5696, 2009. doi:10.1074/jbc.M807632200.
- Wang Y, Jiang F, Wang H, Song T, Wei Y, Yang M, Zhang J, Kang L.** Evidence for the expression of abundant microRNAs in the locust genome. *Sci Rep* 5: 13608, 2015. doi:10.1038/srep13608.
- Wehner R.** Desert ant navigation: how miniature brains solve complex tasks. *J Comp Physiol A Neuroethol Sens Neural Behav Physiol* 189: 579–588, 2003. doi:10.1007/s00359-003-0431-1.
- Wimmer VC, Nevian T, Kuner T.** Targeted in vivo expression of proteins in the calyx of Held. *Pflugers Arch* 449: 319–333, 2004.
- Ylösmäki E, Martikainen M, Hinkkanen A, Saksela K.** Attenuation of Semliki Forest virus neurovirulence by microRNA-mediated detargeting. *J Virol* 87: 335–344, 2013. doi:10.1128/JVI.01940-12.
- Zhu Y, Dewell RB, Wang H, Gabbiani F.** Pre-synaptic muscarinic excitation enhances the discrimination of looming stimuli in a collision-detection neuron. *Cell Reports* 23: 2365–2378, 2018. doi:10.1016/j.celrep.2018.04.079.
- Zhu Y, Gabbiani F.** Combined two-photon calcium imaging and single-ommatidium visual stimulation to study fine-scale retinotopy in insects. In: *Extracellular Recording Approaches*, edited by Sillitoe R. Berlin: Springer, 2018, p. 185–206. doi:10.1007/978-1-4939-7549-5_10.

